

Supplementary Material for *CrystEngComm*

Two Co(II)-based coordination polymers as multi-responsive luminescent
sensors for detection of levofloxacin, benzaldehyde and Fe³⁺ ions in water
media

Ya Liu, Li Ren, Guang-Hua Cui*

*College of Chemical Engineering, Hebei Key Laboratory for Environment Photocatalytic
and Electrocatalytic Materials, North China University of Science and Technology, No. 21 Bohai
Road, Caofeidian new-city, Tangshan, Hebei, 063210, P. R. China*

Corresponding author: Guang-Hua Cui

Fax: +86-0315-8805462. Tel: +86-0315-8805460

E-mail: tscghua@126.com

CONTENTS

Section 1. Experimental Section

Section 2. Supplementary Tables and Structural Figures

Section 1. Experimental Section

1. Materials and physical measurements
2. Synthesis of $[\text{Co}(\text{OBA})(\text{L1})_{0.5}]_n$ (**1**)
3. Synthesis of $[\text{Co}(\text{HBTC})(\text{L2})]_n$ (**2**)
4. X-ray crystallography

1. Materials and physical measurements

L1 and L2 ligands were prepared according to the reported methods [1]. The other solvent and reactants were obtained from commercial sources and applied without purification. Elemental analyses (C, H, and O) of **1** and **2** were performed by a Perkin-Elmer 240C analyzer. The infrared spectra were recorded on a BRUKER VERTEX 80V FT-IR spectrophotometer (400–4000 cm^{-1}). Thermogravimetric analysis (TGA) was conducted on a Netzsch STA449 F1 thermal analyzer at a heating rate of 10 $^{\circ}\text{C min}^{-1}$ from 25 to 700 $^{\circ}\text{C}$ under the air atmosphere protection. The solid-state UV-Vis diffuse-reflectance spectra were measured on a UV-Vis Puxi T9 ultraviolet-visible spectrophotometer with BaSO_4 as the reflection standard. Powder X-Ray Diffraction (PXRD) data was obtained using a Rigaku D/Max-2500PC diffractometer at 40 kV and 40 mA X-ray tube ($\lambda = 1.5418 \text{ \AA}$) on a copper target tube. The luminescence (emission and excitation) spectra were recorded on an Edinburgh instruments FS5 spectrophotometer at the room temperature. An electrochemical workstation (CHI-760D) was used to cyclic voltammetry measurements based on the three-electrode cell.

2. Synthesis of $[\text{Co}(\text{OBA})(\text{L1})_{0.5}]_n$ (**1**)

A mixture of $\text{Co}(\text{OAc})_2 \cdot 4\text{H}_2\text{O}$ (0.2 mmol, 49.8 mg), H_2OBA (0.2 mmol, 96.2 mg), L1 (0.1 mmol, 45.9 mg) and H_2O (10.0 mL) were mixed in a 25 mL Teflon-lined reactor under the autogenous pressure at 140 $^{\circ}\text{C}$ for 72 hours, the reaction mixture was then cooled to room temperature at a rate of 10 $^{\circ}\text{C/h}$. Red blocked crystals of **1** were obtained by filtration and washed with H_2O . Yield: 36.9% based on L1 ligand. Elemental analysis (%) calcd for $\text{C}_{28.5}\text{H}_{21}\text{CoN}_3\text{O}_5$ ($M_r = 544.41$): C, 62.87; H, 3.86; N, 7.72%; found: C, 62.88; H, 3.80; N, 7.81%. IR (cm^{-1}): 1607(s), 1546(m), 1406(m), 1238(s), 1165(w), 891(w), 745(w).

3. Synthesis of $[\text{Co}(\text{HBTC})(\text{L2})]_n$ (**2**)

The experiment procedure of synthesizing **2** is similar to **1**, except using L2 (0.1 mmol, 33.8 mg) to take the place of L1. H_3BTC (0.2 mmol, 42.0 mg) was used instead of H_2OBA . The yield based on the L2 ligand was 37.5%. Elemental analysis (%) calcd. for $\text{C}_{27}\text{H}_{20}\text{CoN}_4\text{O}_6$ ($M_r = 555.40$): C, 58.38; H, 3.60; N, 10.09%; found: C, 58.27; H, 3.65; N, 10.12%. IR (cm^{-1}): 1618(s), 1562(m), 1512(w), 1434(w), 1372(s), 763(m), 719(w).

4. X-ray crystallography

The single-crystal structures of the **1/2** were measured at the Rigaku XtaLAB mini

diffractometer equipped with MoK α radiation ($\lambda = 0.71073 \text{ \AA}$) at 100 k. Integration, absorption correction, and determination of unit cell parameters were processed using the CrysAlisPro program (version 1.171.38.41). The two structures were solved by the intrinsic phasing method (SHELXT-2015) and further refined using the full-matrix least square method on F^2 (SHELXL-2018). All of the non-hydrogen atoms were refined using full-matrix least squares methods with anisotropic thermal parameters. The positions of hydrogen atoms were fixed geometrically at calculated distances and is tropically refined *via* the riding model. The crystallographic data and structure determination statistics for two CPs are summarized in Table S1. Table S2 lists the selected necessary bond distances and angles.

5. Experimental section

5.1 Sensing of antibiotics

In order to evaluate selectivity and sensitivity of **1** and **2** to some common antibiotics, including Amoxicillin (AMX), Ciprofloxacin (CIP), enrofloxacin (ENR), Levofloxacin (LEV), metronidazole (MTR), Norfloxacin (NOR), furantoin (NIT), ornidazole (ORN), pefloxacin (PEF), ronidazole (RNZ), sulfadiazine (SDZ), sulfamethazine (SMZ), sulfamethoxazole (SMX), nitrofurantoin (SEM), and tetracycline (TE). 4.0 mg finely grinded powders of **1** or **2** were dispersed into 4 mL H₂O, creating the suspension solution under ultrasonic vibration. Further, 400 μ L different antibiotic (1×10^{-4} mol/L) were slowly dropped into the solution and irradiated ultrasonically again. The blank experiments were also disposed by using the suspension of the samples in water and treat it under the same requirement. [The resulting suspensions were promptly used for the measurements of fluorescence recognition. Interference experiments were carried out, introducing LEV, other antibiotics into, and aqueous solutions \(c:c = 1:1\) of 1/2 to form suspensions \(4 mL\).](#)²

5.2 Sensing of small organic molecules

CPs as the fluorescence probes are increasingly applied in detection various organic molecules, the solvent emulsions were obtained by taking 4 mg powder of **1** and **2** into 4 mL solutions of benzaldehyde (BZH), *n*-butanol (BuOH), cyclohexane (CHX), dimethylformamide (DMF), N,N-dimethylacetamide (DMA), dimethyl sulfoxide (DMSO), dichloromethane (DCM), N-methyl pyrrolidone (NMP), ethylene glycol (EG), ethanol (EtOH), formaldehyde (FA), Glyoxal (GO), acetonitrile (MeCN), methanol (MeOH), N-methyl pyrrolidone (NMP), [and the distribution of 1 and 2 in aqueous solution as the blank test. The final mixtures were sonicated for 30 minutes, and](#)

were performed in the luminescence experiments immediately. Anti-interference tests were conducted in the existence of BZH (2 mL) and other organics (2 mL) under the same conditions.

5.3 Sensing of metal ions

As for cations, the suspensions were equipped by adding the samples of **1/2** (4 mg) in the solutions of 4 mL aqueous solutions containing various nitrates ($M(NO_3)_x$, $M = Na^+, K^+, Mg^{2+}, Ca^{2+}, Sr^{2+}, Ba^{2+}, La^{3+}, Sm^{3+}, Eu^{3+}, Gd^{3+}, Tb^{3+}, Er^{3+}, Cr^{3+}, Fe^{3+}, Co^{2+}, Ni^{2+}, Cu^{2+}, Ag^+, Zn^{2+}, Cd^{2+}, Hg^{2+}, Al^{3+}$ and Pb^{2+}) with the concentration of 5×10^{-4} mol/L. It can be regard as the blank experiment, when the metal ions are non-existent. The resulting suspensions were ultrasonicated for 30 min and used for fluorescence experiments. Interference experiments were implemented in the presence of Fe^{3+} ions and other metal ions with the identical concentration.

- [1] M.M. Chen, L. Chen, H.X. Li, L. Brammer and J.P. Lang, *Inorg. Chem. Front.*, 2016, **3**, 1297–1305.
- [2] J.H. Qin, H.R. Wang, M.L. Han, X.H. Chang and L.F. Ma, *Dalton Trans.*, 2017, **46**, 15434–15442.

We calculate the detection limit based on the reported literature.^{3,4,5} The specific process is as follows:

$$\sigma = \sqrt{\frac{\sum_{i=1}^n (x_i - \bar{x})^2}{n-1}}$$

$$k = \frac{I}{c}$$

$$DL = \frac{3\sigma}{k}$$

σ is the slope of the calibration curve; k is the standard deviation for replicating detections of blank solutions.

Taking calculation limit of **1/2** for LEV:

$$K = 5.07 \times 10^3 \text{ M}^{-1}, \sigma = 0.0082 \text{ (n = 10)}, DL = 3 \times 0.0082 / (5.07 \times 10^3) = 4.83 \times 10^{-6} \text{ M}$$

$$K = 2.03 \times 10^3 \text{ M}^{-1}, \sigma = 0.0067 \text{ (n = 10)}, DL = 3 \times 0.0067 / (2.03 \times 10^3) = 9.86 \times 10^{-6} \text{ M}$$

The calculation limit of **1/2** for BZH:

$$K = 1.09 \times 10^3 \text{ M}^{-1}, \sigma = 0.0082 \text{ (n = 10)}, DL = 3 \times 0.0082 / (1.09 \times 10^3) = 2.23 \times 10^{-6} \text{ M}$$

$$K = 1.90 \times 10^3 \text{ M}^{-1}, \sigma = 0.0067 \text{ (n = 10)}, DL = 3 \times 0.0067 / (1.90 \times 10^3) = 1.05 \times 10^{-6} \text{ M}$$

The calculation limit for Fe^{3+} ions:

$$K = 3.54 \times 10^3 \text{ M}^{-1}, \sigma = 0.0082 \text{ (n = 10)}, DL = 3 \times 0.0082 / (3.54 \times 10^3) = 6.92 \times 10^{-6} \text{ M}$$

$$K = 1.97 \times 10^3 \text{ M}^{-1}, \sigma = 0.0067 \text{ (n = 10)}, DL = 3 \times 0.0067 / (1.97 \times 10^3) = 10.16 \times 10^{-6} \text{ M}$$

References:

- [3] H. Xu, J. Gao, X. Qian, J. Wang, H. He, Y. Cui, Y. Yang, Z. Wang and G. Qian, *J. Mater. Chem. A.*, 2016, 4, 10900-10905.
- [4] C. L. Zhang, Z. T. Liu, H. Xu, H. G. Zheng, J. Ma and J. Zhao, *Dalton Trans.*, 2019, 48, 2285-2289.
- [5] T. Wiwasuku, J. Boonmak, K. Siriwong, V. Ervithayasuporn, S. Youngme, *Sensor. Actuat. B-Chem.*, 2019, 284, 403-413.

Section 2. Supplementary Tables and Structural Figures

Table Titles:

Table S1 Crystallographic data and refinement parameter for **1** and **2**.

Table S2 Selected bond lengths (Å) and angles (°) for **1** and **2**.

Table S3 Comparison of the sensitivities of **1** and **2** for LEV with related Materials.

Table S4 Comparison of the sensitivities of **1** and **2** for BZH with related CPs.

Table S5 Comparison of the sensitivities of **1** and **2** with previously reported CPs to Fe³⁺ ions.

Table S1 Crystallographic data and refinement parameter for **1** and **2**

CPs	1	2
Chemical formula	C _{28.50} H ₂₁ CoN ₃ O ₅	C ₂₇ H ₂₀ CoN ₄ O ₆
Formula weight	544.41	555.40
Crystal system	Monoclinic	Monoclinic
Space group	<i>C2/c</i>	<i>C2/c</i>
<i>a</i> (Å)	12.6009(6)	17.714(1)
<i>b</i> (Å)	30.1566(12)	17.989(1)
<i>c</i> (Å)	13.5693(8)	15.344(1)
α (°)	90	90
β (°)	107.237(6)	105.098(1)
γ (°)	90	90
<i>V</i> (Å ³)	4924.8(5)	4721(5)
<i>Z</i>	2	8
<i>D</i> _{calcd} (g/cm ³)	1.469	1.563
Absorption coefficient, mm ⁻¹	0.743	0.781
<i>F</i> (000)	2240	2280
Crystal size, mm	0.22×0.19×0.18	0.16×0.15×0.11
θ range, deg	2.120–30.550	1.643–27.561
Index range <i>h, k, l</i>	–18/17, –42/42, –17/19	–21/22, –23/12, –19/17
Reflections collected	34515	14123
Independent reflections (<i>R</i> _{int})	7162(0.0397)	5359(0.0477)
Data/restraint/parameters	7162/0/340	5359/0/343
Goodness-of-fit on <i>F</i> ²	1.025	0.839
Final <i>R</i> ₁ , <i>wR</i> ₂ (<i>I</i> > 2σ(<i>I</i>))	0.0422, 0.1104	0.0444, 0.1445
Largest diff. peak and hole	1.180, –0.830	0.461, –0.404

Table S2 Selected bond lengths (Å) and angles (°) for **1** and **2**

Parameter	Value	Parameter	Value
CP 1			
Co(1)–O(1)	1.954(2)	Co(1)–N(1)	2.036(2)
Co(1)–O(1)A	1.954(2)	Co(1)–N(1)A	2.036(2)
Co(2)–O(5)B	2.084(2)	Co(2)–N(3)	2.106(2)
Co(2)–O(5)C	2.084(2)	Co(2)–N(3)D	2.106(2)
Co(2)–O(4)B	2.235(2)	Co(1)–O(4)C	2.235(2)
O(1)–Co(1)–O(1)A	101.59(1)	O(1)A–Co(1)–N(1)A	106.88(7)
O(1)–Co(1)–N(1)	106.88(7)	O(1)–Co(1)–N(1)A	113.65(8)
O(1)A–Co(1)–N(1)	113.65(8)	N(1)–Co(1)–N(1)A	113.69(1)
O(5)B–Co(2)–O(5)C	161.34(1)	O(4)C–Co(2)–O(5)C	60.51(8)
O(4)C–Co(2)–O(5)C	107.25(8)	O(4)B–Co(2)–O(5)B	60.51(8)
O(4)B–Co(2)–O(5)C	107.25(8)	O(4)B–Co(2)–O(4)C	105.78(1)
N(3)–Co(2)–O(5)C	99.70(7)	N(3)D–Co(2)–O(5)C	93.41(7)
N(3)–Co(2)–O(5)B	93.41(7)	N(3)D–Co(2)–O(5)B	99.70(7)
N(3)D–Co(2)–O(4)C	153.05(8)	N(3)–Co(2)–O(4)C	87.55(8)
N(3)D–Co(2)–O(4)B	87.55(8)	N(3)–Co(2)–O(4)B	153.05(8)
N(3)–Co(2)–N(3)D	90.64(1)		
CP 2			
Co(1)–O(1)	2.029(2)	Co(1)–O(2)A	2.028(2)
Co(1)–N(1)	2.138(3)	Co(1)–N(4)B	2.153(3)
Co(1)–O(3)C	2.162(2)	Co(1)–O(4)C	2.278(3)
O(2)A–Co(1)–O(1)	121.37(9)	O(2)A–Co(1)–N(1)	88.69(1)
O(1)–Co(1)–N(1)	91.41(9)	O(2)A–Co(1)–N(4)B	92.26(1)
O(1)–Co(1)–N(4)B	83.96(9)	N(1)–Co(1)–N(4)B	175.07(9)
O(2)A–Co(1)–O(3)C	87.49(9)	O(1)–Co(1)–O(3)C	151.10(8)
N(1)–Co(1)–O(3)C	90.62(9)	N(4)B–Co(1)–O(3)C	94.25(9)
N(4)B–Co(1)–O(4)C	93.88(8)	O(1)–Co(1)–O(4)C	92.31(8)
O(2)A–Co(1)–O(4)C	146.23(8)	O(3)C–Co(1)–O(4)C	58.95(8)
N(1)–Co(1)–O(4)C	88.00(8)		

Symmetry codes for **1**: A = $-x, +y, 3/2-z$; B = $-1/2+x, 1/2+y, +z$; C = $3/2-x, 1/2+y, 3/2-z$, D = $1-x, +y, 3/2-z$. for

2: A = $-x+1, y, -z+1/2$, B = $x-1/2, y-1/2, z$, C = $x+1/2, -y+3/2, z+1/2$.

Table S3 Comparison of the sensitivities of **1** and **2** for LEV with related Materials

Materials	LOD/M	Ref
levofloxacin–silver nanoparticles	6.0×10^{-9}	[6]
Eu@TpPa-1	6.0×10^{-7}	[7]
Tb@TFP-EB	1.2×10^{-6}	[8]
1	4.83×10^{-6}	This work
2	9.86×10^{-6}	This work

Pa-1 = *p*-Phenylenediamine; TFP = 2,4,6-Trihydroxy-benzene-1,3,5-tricarbaldehyde.

Table S4. Comparison of the sensitivities of **1** and **2** for BZH with related CPs

CPs	LOD/M	Ref
$[\text{Co}(\text{TBTA})(\text{L1})_2]_n$	3.43×10^{-6}	[9]
$[\text{Co}(\text{TBTA})(\text{L3})_{1.5}]_n$	3.11×10^{-6}	[9]
$\{[\text{Co}_2(\text{BTC})(\text{L})] \cdot 0.25\text{H}_2\text{O}\}_n$	2.10×10^{-6}	[10]
$[\text{Ag}(\text{HIPA})(\text{L})]_n$	9.68×10^{-6}	[10]
1	2.23×10^{-6}	This work
2	1.05×10^{-6}	This work

H₂TBTA = tetrabromoterephthalic acid, L1 = 1,2-bis(benzimidazol-1-ylmethyl)benzene, L3 = 1,4-bis(benzimidazol-

1-ylmethyl)benzene, H₄BTC = 1,2,3,4-butanetetracarboxylic acid, L = 1,6-bis(5,6-dimethylbenzimidazol-1-

yl)hexane), H₂IPA = isophthalic acid.

Table S5. Comparison of the sensitivities of **1** and **2** with previously reported CPs toFe³⁺ ions

CPs	LOD/M	Ref
{[Co ₂ (BTC)(L)]·0.25H ₂ O} _n	3.30×10 ⁻⁶	[10]
[Cd _{0.5} (TBTA) _{0.5} (L1)] _n	2.64×10 ⁻⁵	[11]
[Cd(TBTA)(L2)(H ₂ O)] _n	5.62×10 ⁻⁶	[11]
1	6.92×10 ⁻⁶	This work
2	1.01×10 ⁻⁵	This work

H₄BTC = 1,2,3,4-butanetetracarboxylic acid, L = 1,6-bis(5,6-dimethylbenzimidazol-1-yl)hexane), L1 = 1,3-bis(2-methylbenzimidazol-1-yl)-2-propanol, H₂TBTA = tetrabromoterephthalic acid, L2 = 1,2-bis(benzimidazol-1-ylmethyl)benzene.

[6] T.D. Smirnova, T.G. Danilina, T.Yu. Rusanova and N.A. Simbireva, *J. Anal. Chem.*, 2021, 76, 89–94.

[7] J.M. Wang, X. Lian and B. Yan, *Inorg. Chem.*, 2019, 58, 9956–9963.

[8] X. Liang, H.M. Liu, Y. Du, W.Z. Li, M. Wang, B. Ge and L.M. Zhao, *Colloid. Surface. A.*, 2020, 606, 125429.

[9] A.L. Li, Y.H. Qua, L.S. Fu, C. Han and G.H. Cui, *CrystEngComm*, 2020, 22, 2656–2666.

[10] A.L. Li, Z.C. Hao, C. Han and G.H. Cui., *Appl. Organometal. Chem.*, 2020, 34, e5313.

[11] Y. Liu, C. Han and G.H. Cui, *Inorg. Chim. Acta.*, 2021, 525, 120499.

Figure Titles:

Fig. S1 TGA plots of **1** and **2**.

Fig. S2 Simulated and experimental PXRD patterns for **1** and **2**.

Fig. S3 (a) The PXRD patterns of **1** in different pH solutions; (b) The PXRD patterns of **2** in different pH solutions.

Fig. S4 The change of the fluorescence emission intensity of **1** and **2** in different pH solutions.

Fig. S5 Solid luminescence lifetime of **1** (a) and **2** (b).

Fig. S6 Time-dependent emission spectra of **1** (a) and **2** (b) suspended in aqueous solutions.

Fig. S7 Anti-interference experiments of **1** and **2** for LEV with other antibiotics.

Fig. S8 Comparison of the luminescence intensity of **1** (a) and **2** (b) in the presence of mixed organic solvents.

Fig. S9 Fluorescence emission spectra of Fe^{3+} ions and other metal ions in **1** (a) and **2** (b).

Fig. S10 (a) Reversibility of **1** for the detection of LEV; (b) Reversibility of **2** for the detection of LEV; Reversibility of **1** (c) and **2** (d) for the detection of BZH; Reversibility of **1** (e) and **2** (f) for the detection of Fe^{3+} ions.

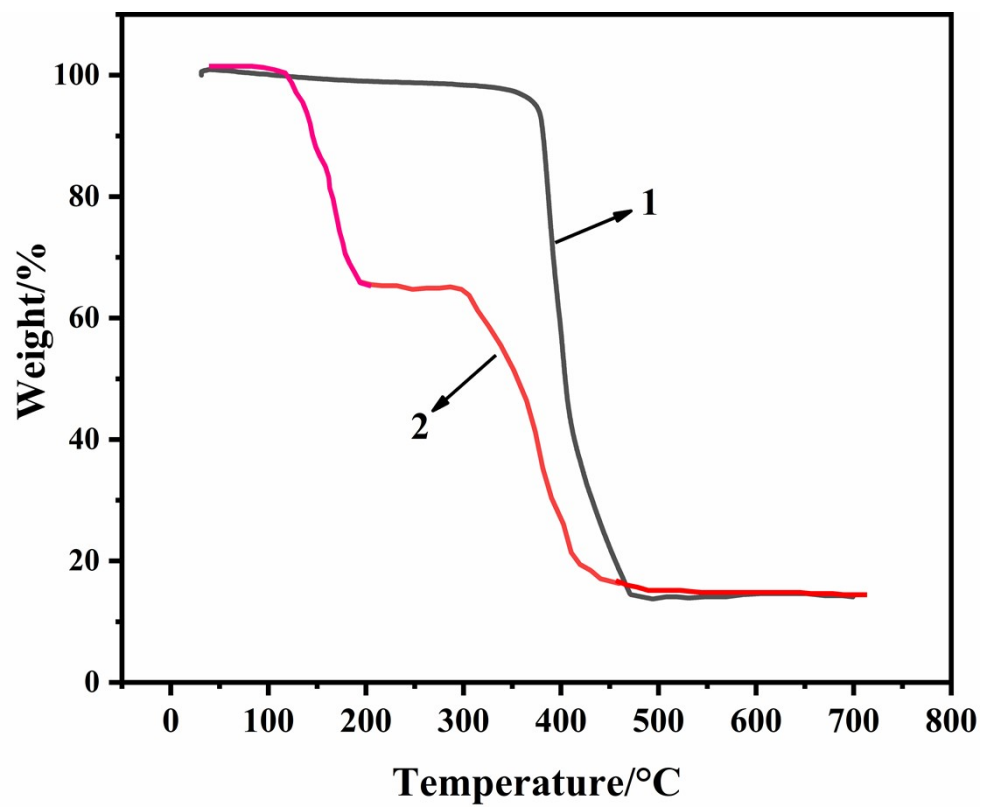


Fig. S1 TGA plots of 1 and 2.

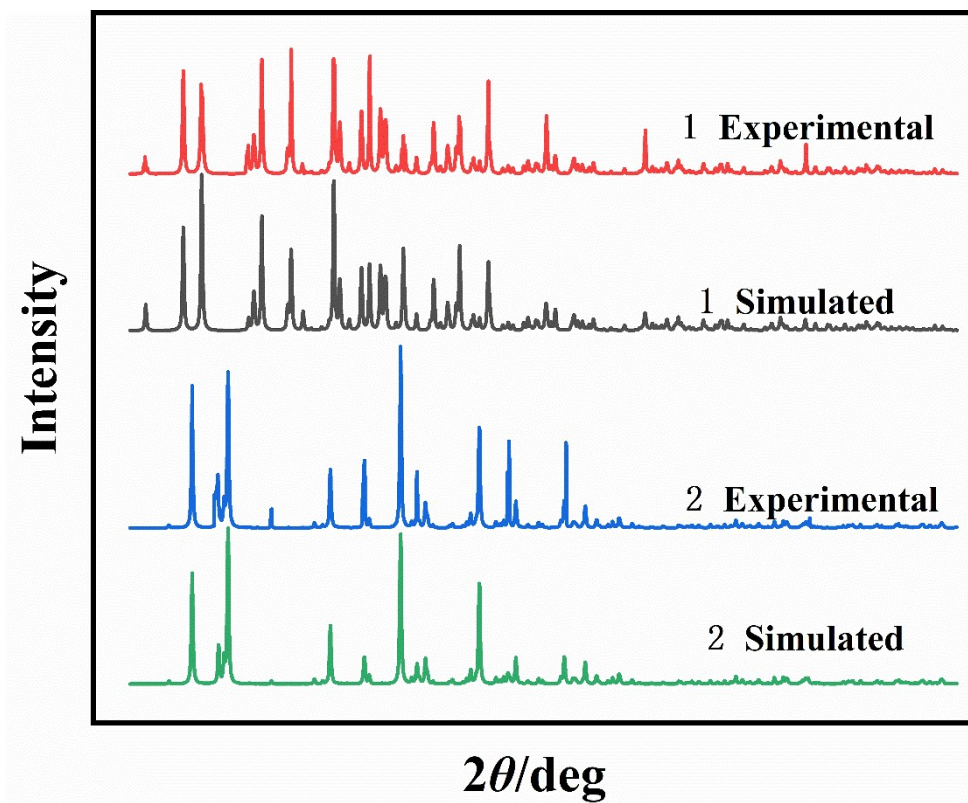
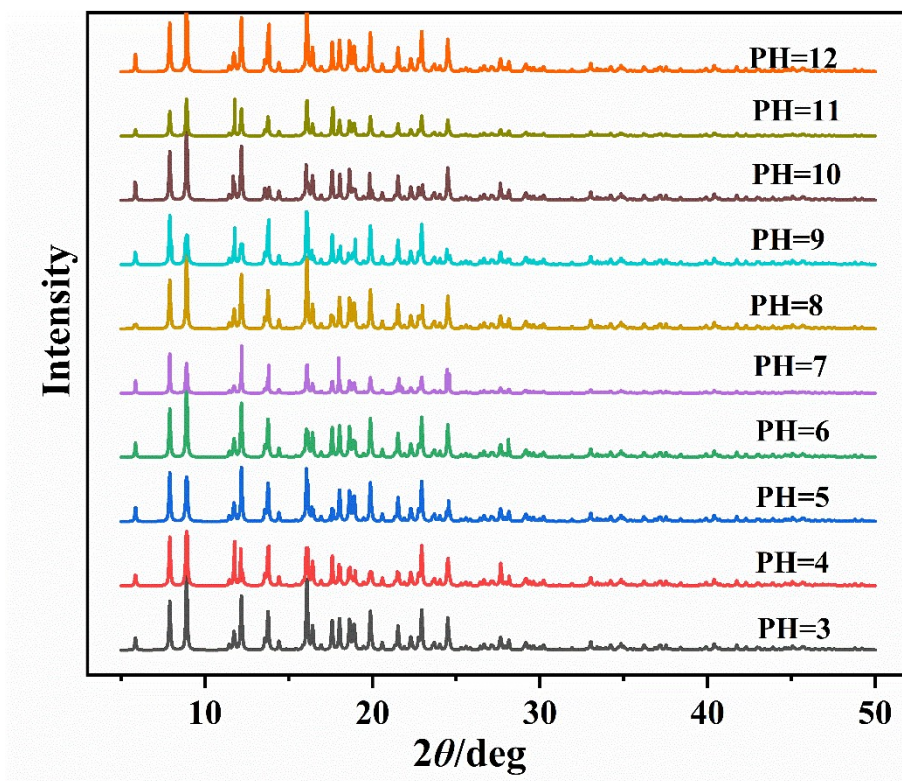
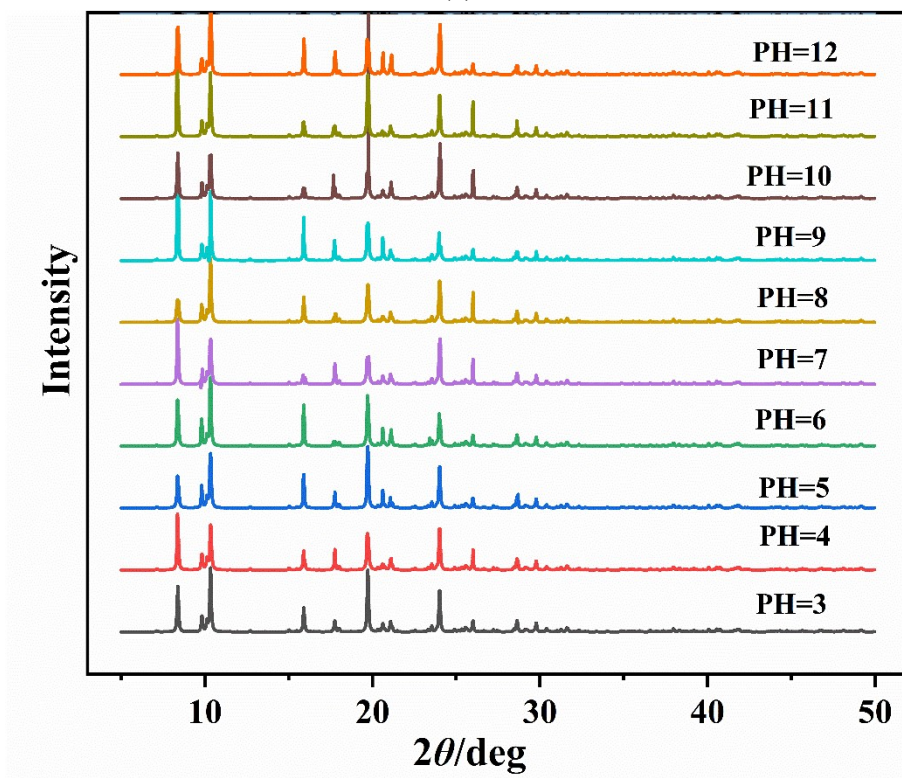


Fig. S2 Simulated and experimental PXRD patterns for 1 and 2.



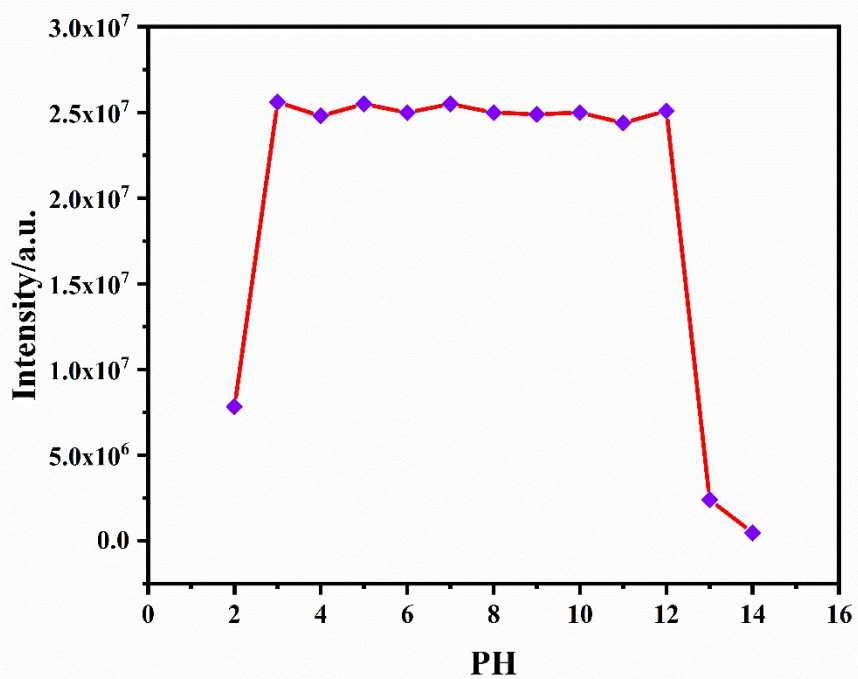
(a)



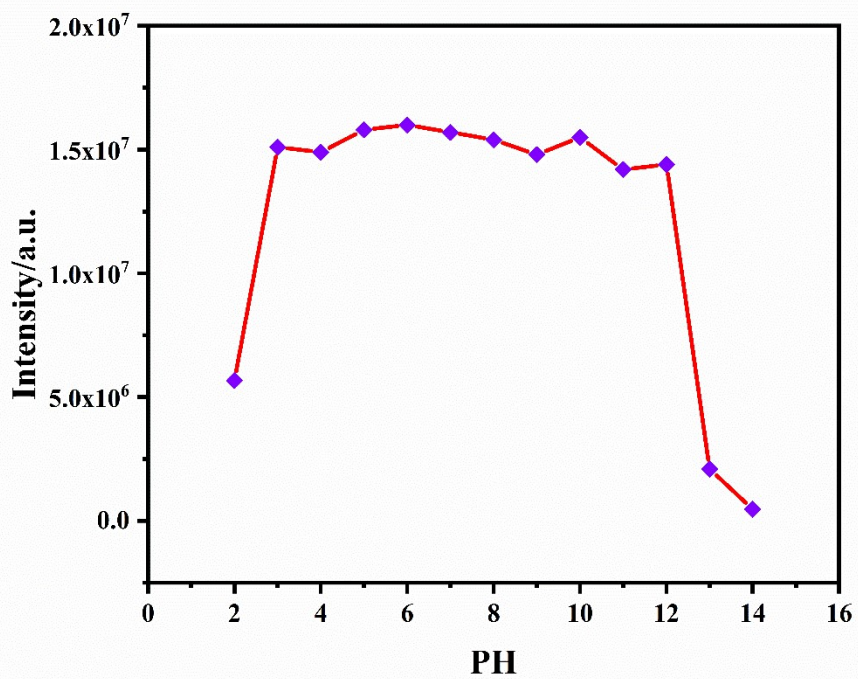
(b)

Fig. S3 (a)The PXRD patterns of 1 in different pH solutions; (b) The PXRD patterns of 2 in different pH

solutions.

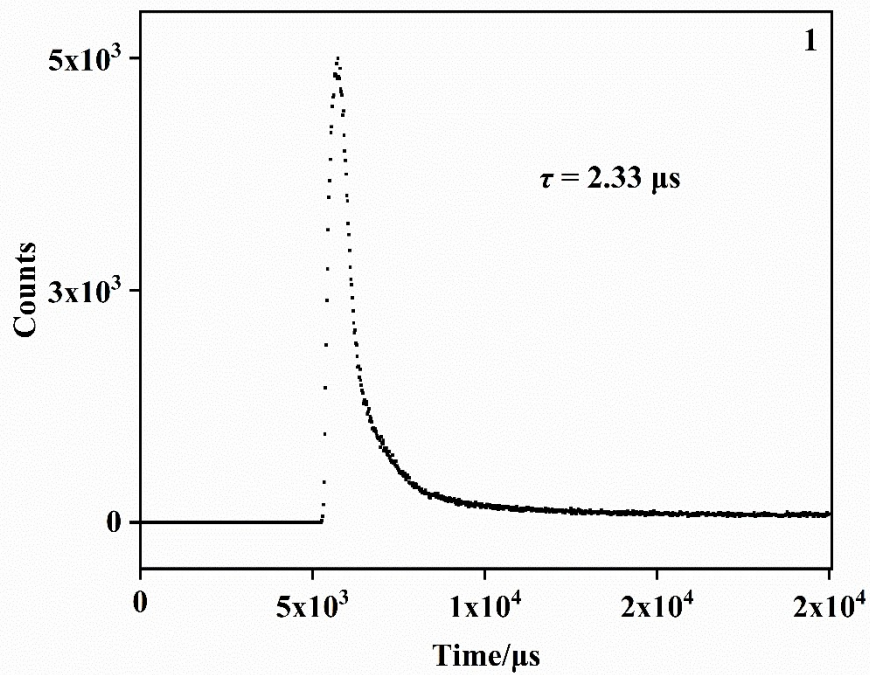


(a)

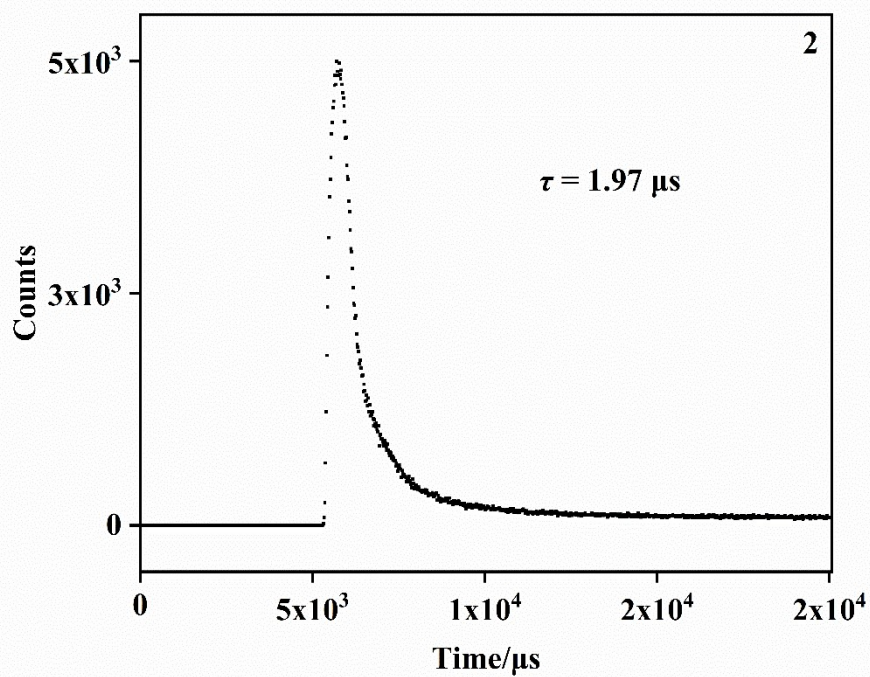


(b)

Fig. S4 The change of the fluorescence emission intensity of 1 (a) and 2 (b) in different pH solutions.

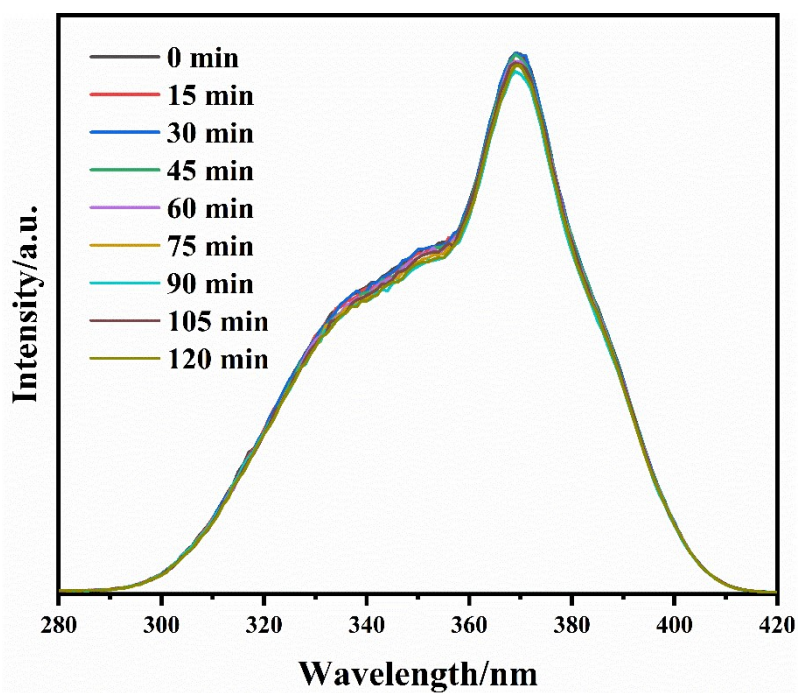


(a)

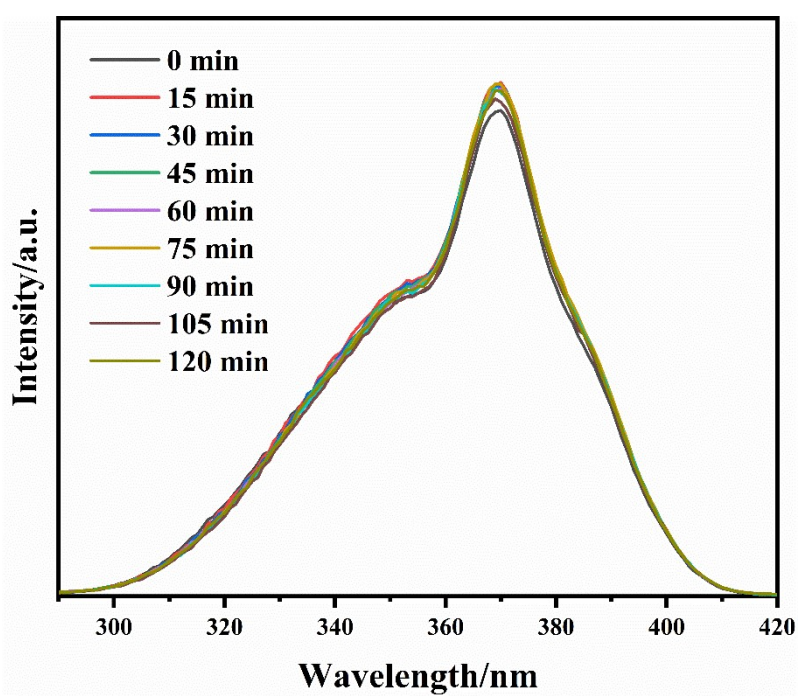


(b)

Fig. S5 Solid luminescence lifetime of 1 (a) and 2 (b).

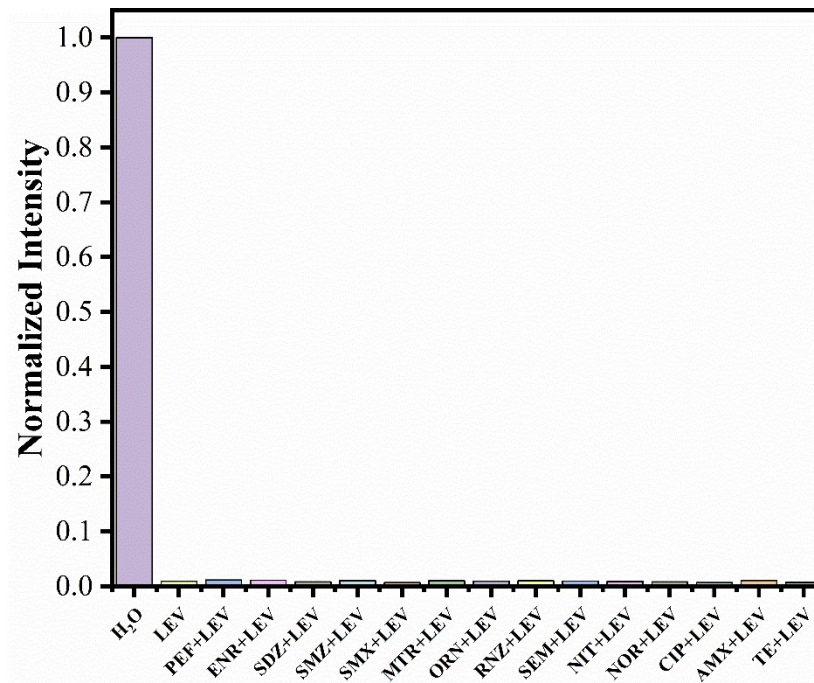


(a)

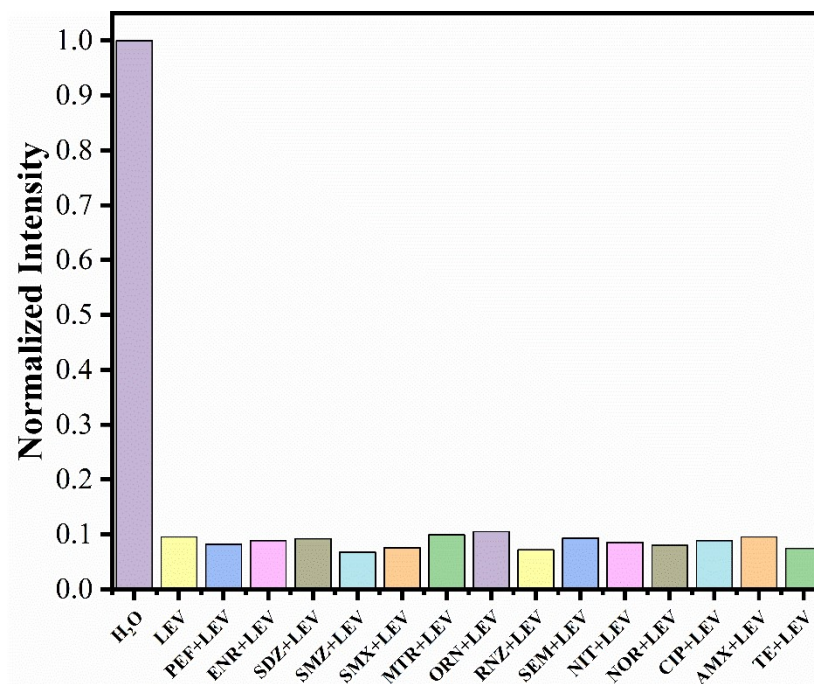


(b)

Fig. S6 Time-dependent emission spectra of 1 (a) and 2 (b) suspended in aqueous solutions.

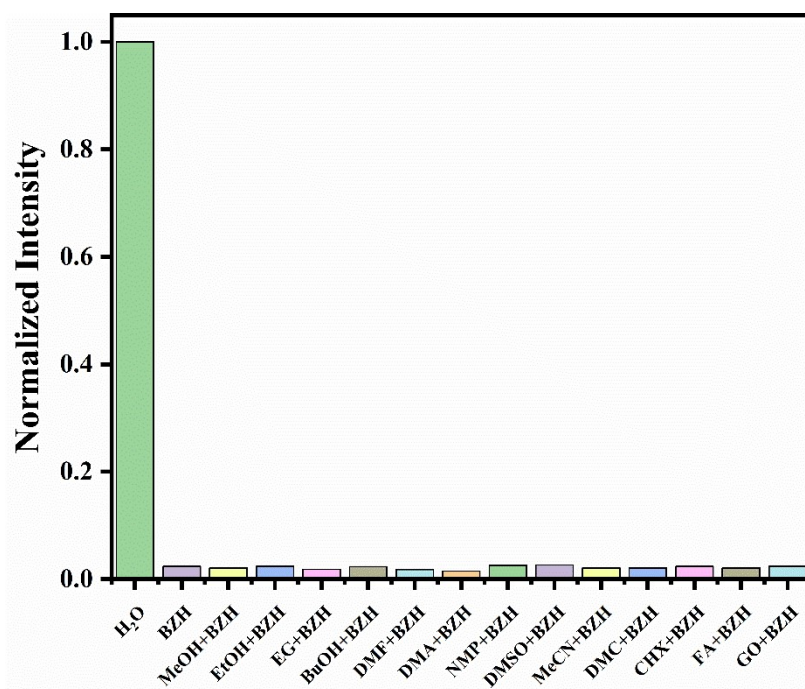


(a)

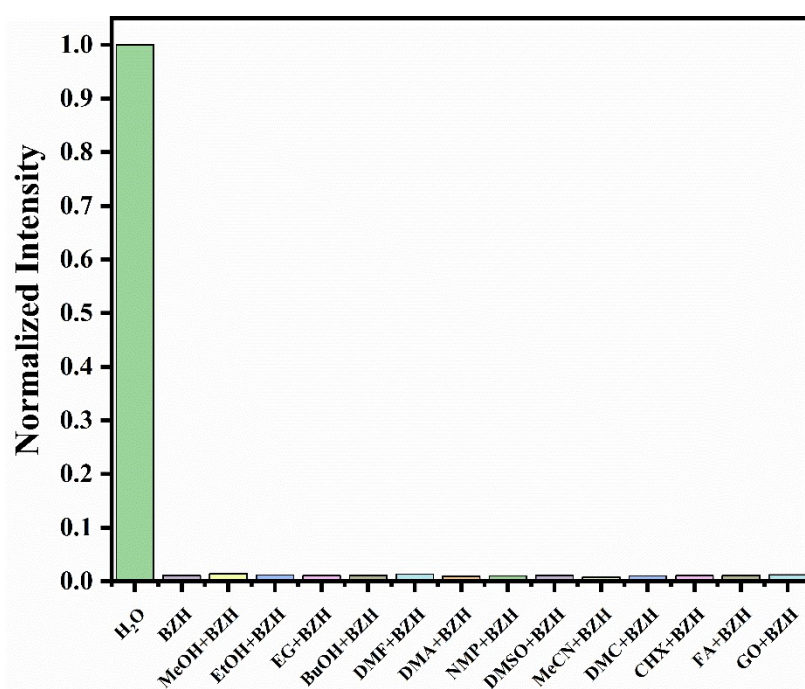


(b)

Fig. S7 Anti-interference experiments of 1 and 2 for LEV with other antibiotics.

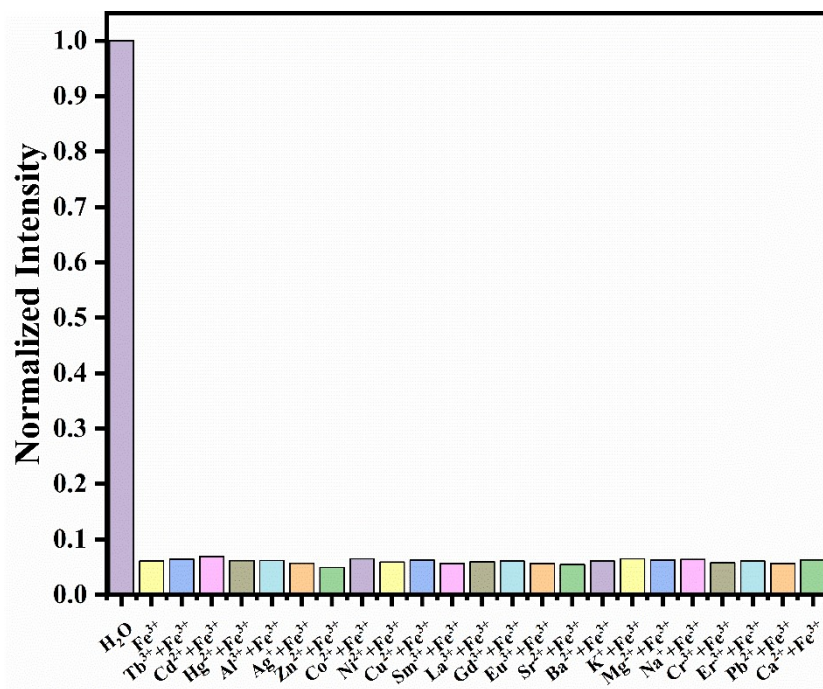


(a)

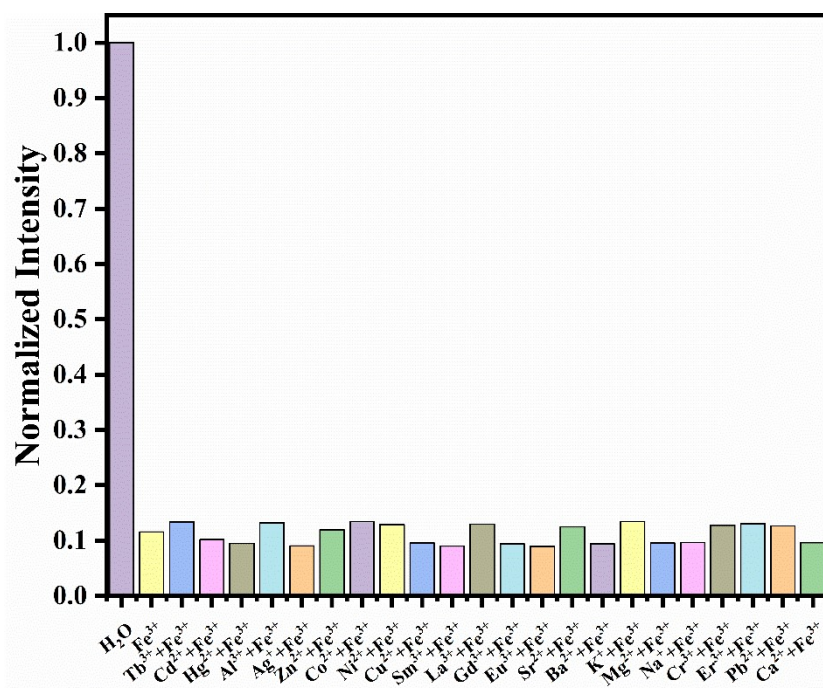


(b)

Fig. S8. Comparison of the luminescence intensity of 1 (a) and 2 (b) in the presence of mixed organic solvents.



(a)



(b)

Fig. S9. Fluorescence emission spectra of Fe³⁺ ions and other metal ions in **1** (a) and **2** (b).

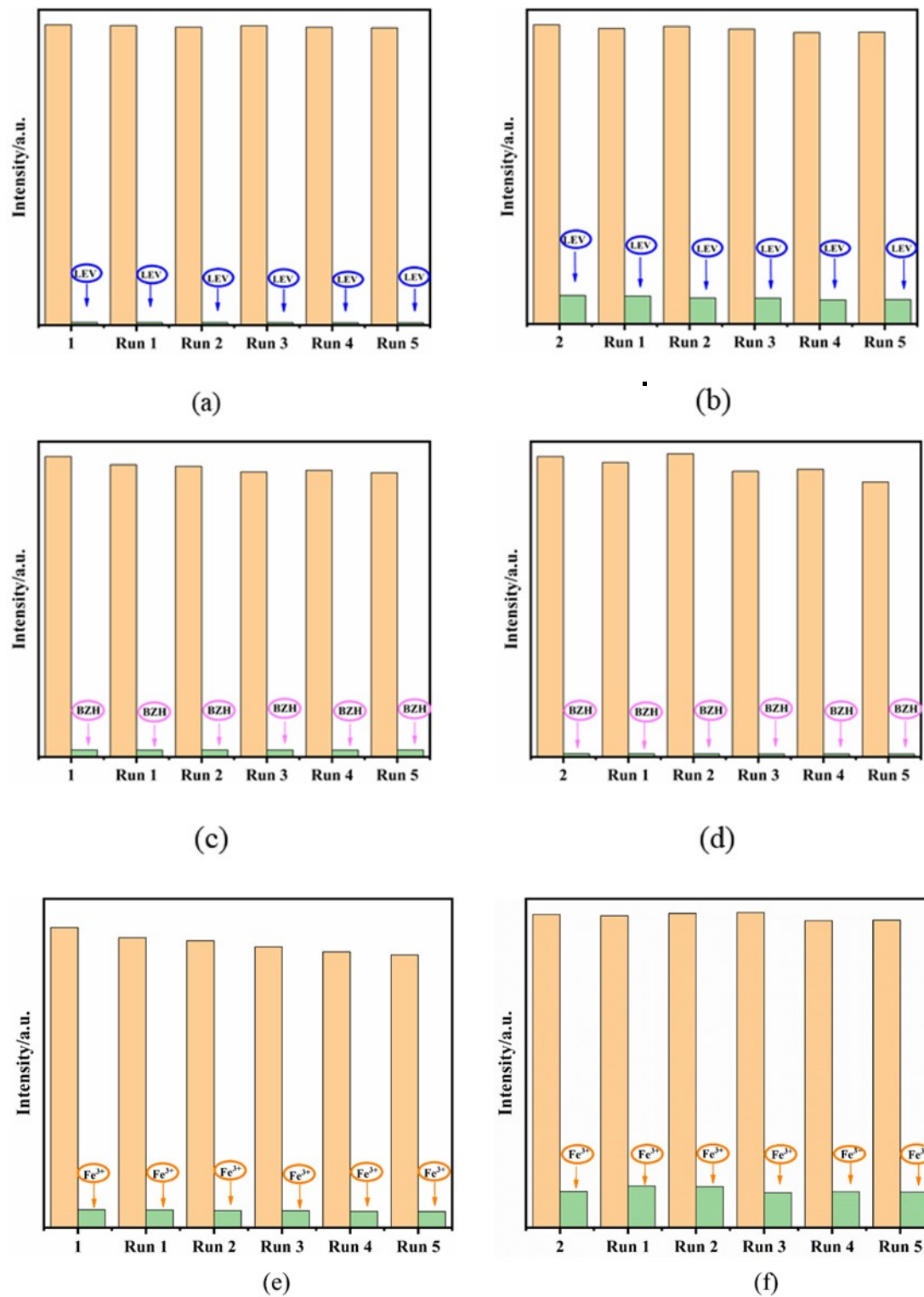


Fig. S10 (a) Reversibility of **1** for the detection of LEV; (b) Reversibility of **2** for the detection of LEV; Reversibility of **1** (c) and **2** (d) for the detection of BZH; Reversibility of **1** (e) and **2** (f) for the detection of Fe³⁺ ions.